Twenty-Seventh Symposium (International) on Combustion/The Combustion Institute, 1998/pp. 3197–3204

LASEROPTICAL INVESTIGATION OF HIGHLY PREHEATED COMBUSTION WITH STRONG EXHAUST GAS RECIRCULATION

TOBIAS PLESSING,[1] NORBERT PETERS,[1] AND JOACHIM G. WÜNNING[2]
[1]*Institut für Technische Mechanik*
RWTH-Aachen
Templergraben 64
D-52056 Aachen, Germany
[2]*WS-Wärmeprozesstechnik*
DornierStr. 14
D-71272 Renningen, Germany

Laseroptical measurements using OH laser-induced predissociative fluorescence and Rayleigh thermometry were carried out in a combustion chamber with highly preheated air and strong exhaust gas recirculation. Under these conditions, combustion takes place without any luminousity and is referred to as flameless oxidation. It is realized by a configuration with exhaust gas recirculation that is entrained by air nozzles operating as a jet pump. This leads to low temperatures even at significant air preheating so that thermal NO formation is largely suppressed.

In the optically accessible combustion chamber, the reaction zones of flameless oxidation were visualized, and burning and mixing regions were identified. The instantaneous flame structure is compared to measurements in turbulent premixed flames. Only disconnected reaction zones due to strong flame stretch resulting from high flow velocities were observed. In the flowfield ahead of the burner, fresh gas was mixed with the hot exhaust gases. The fresh gas was diluted and heated up simultaneously. Flameless oxidation could only be observed if the temperature of the unburnt mixture was above 950 K. The temperature rise between the unburnt and burnt side of the reaction zones varied between 200 and 400 K, depending on the dilution of the unburnt mixture with exhaust gases. This temperature rise was compared with a theoretical analysis of a temperature equation for the well-stirred reactor. It can be shown that flameless oxidation takes place in the well-stirred reactor regime. Maximum local temperatures below 1650 K were measured. The OH concentration in the combustion zones of flameless oxidation is lower than in non-preheated undiluted turbulent premixed flames.

Introduction

For high-temperature process heating, a better efficiency is often achieved by air preheating [1]. Energy from the exhaust gases is transferred back to the combustion air in recuperative or regenerative heat exchangers. A negative consequence of air preheating is increased peak flame temperatures with a strong effect on thermal NO formation. To overcome the trade-off between energy saving and NO reduction, the temperature within the combustion zone needs to be as low as possible. Staged combustion, exhaust gas recirculation, or other flame cooling methods are applied to lower the combustion temperatures [2]. For burner-stabilized flames, exhaust gas recirculation is limited, and often flames are cooled at the outer edge, so that thermal NO formation is only partially reduced. For non-burner-stabilized combustion, much more exhaust gases can be fed back to the combustion zone. A new combustion arrangement, referred to as flameless oxidation [3], uses a combination of strong internal exhaust gas recirculation with preheating of the fuel air mixture and non-burner-stabilized combustion. By internal exhaust gas recirculation, the temperature rise within the reaction zone is significantly lowered. Characteristic features of this combustion mode are no emission of sound, no visible flame, and barely any NO formation.

Because no visible flame can be seen, it was so far unclear where reaction takes place such that combustion control is difficult. Therefore, reaction zones are visualized in this study with two-dimensional laser-induced predissociative fluorescence of the OH radical (OH-LIPF). Simultaneously, temperatures are measured by Rayleigh scattering for an identification of the combustion zones and for an analysis of the structure of flameless oxidation. The results are compared with measurements in turbulent stoichiometric premixed methane bunsen flames.

Flameless Oxidation

In contrast to combustion in stabilized flames, flameless oxidation is a nonstabilized combustion

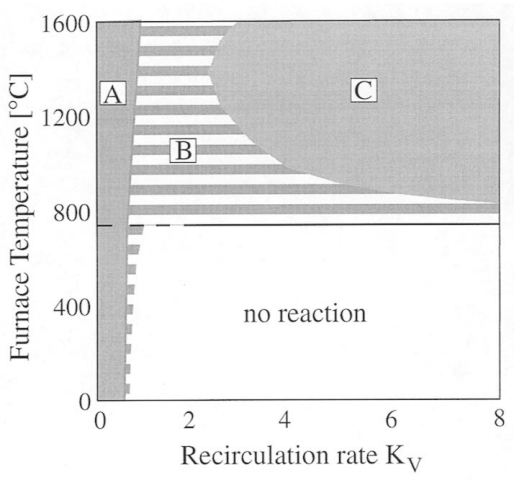

FIG. 1. Definition of stability areas as a function of exhaust gas recirculation and furnace temperature.

that is mixing controlled and is achieved by specific flow and temperature conditions. Flameless oxidation is primarily based on the dilution of the unburnt gases as a very effective method to lower peak flame temperatures, resulting in lowered NO emissions. Preheating of the primary air enhances the efficiency without affecting the NO emissions. Exhaust gases are recirculated internally in three stages. Mixing of air and exhaust gases is followed by addition of fuel to the diluted air. Finally, a non-burner-stabilized combustion, referred to as flameless oxidation, takes place, in which exhaust gases are again internally recirculated. Preheating of air is not a necessary requirement for flameless oxidation because exhaust gas recirculation dominates the process of heating up unburnt gases. There is no combustion noise, NO emissions are very low even at high preheating temperatures of the primary air, and there is no visible reaction.

The most important difference to conventional flames is the very high exhaust gas recirculation. The recirculation rate is defined as

$$K_V = \frac{\dot{M}_E}{\dot{M}_F + \dot{M}_A} \tag{1}$$

where E is recirculated exhaust gas, F is fuel, and A is combustion air. To provide reliable operating conditions in conventional systems, exhaust gas recirculation rates of $K_V \leq 0.3$ are used as a NO_x-reducing technique. Under special conditions [3], a stable form of combustion is also possible for much higher recirculation rates. Fig. 1 shows a schematic diagram of the stability limits for different combustion modes. Stable flames (A) are possible over the whole range of combustion chamber temperatures, but only for recirculation rates up to 30% (somewhat increased at higher temperatures). For higher recirculation rates, the flame becomes unstable (B), lifts off, and finally blows out (for temperatures below self-ignition). If, however, the furnace temperature and the exhaust gas recirculation are sufficiently high ($K_V \geq 3.0$), the fuel can react in the very steady, stable form of flameless oxidation (C). As can be seen from the diagram, it is not possible to operate a burner with flameless oxidation in a cold combustion chamber. Therefore, the combustion chamber must be heated up with undiluted burner-stabilized flames before it can be switched to flameless oxidation.

In theory, flameless oxidation has a little temperature rise in the reaction zone and comes very close to the model of a well-stirred reactor, because turbulent timescales are much smaller than chemical timescales due to the very strong dilution of the premixture. In a well-stirred reactor, the temperature for ignition and extinction can be described as a steady-state solution [4]:

$$T^*_{I,Q} = \frac{(2 + Q^*) \pm Q^*\sqrt{1 - 4(1 + Q^*)/E^*Q^*}}{2(1 + Q^*)/E^*} \tag{2}$$

T^* denotes a nondimensional temperature $T^* = T/T_u$, Q^* a nondimensional heat of combustion $Q^* = (T_b - T_u)/T_u$, and E^* a nondimensional activation energy $E^* = E/RT_u$. T_b is the temperature in the burnt (equilibrium adiabatic flame temperature) and T_u in the unburnt gases. For sufficiently large values of E^*, the quadratic equation 2 has two solutions, one for ignition and one for quenching. The result is the well-known S-shaped curve. The temperatures for ignition and extinction coincide if $E^* = 4(1 + Q^*)/Q^*$, and for $E^* < 4(1 + Q^*)/Q^*$, the S-shaped curve develops into a monotonous transition between burnt and unburnt gases. For this case, the temperature rise in the reaction zone $\Delta T \leq 4RT_uT_b/E$ can be solved iteratively with $E/R \approx 20000$ K. This leads to the solid line shown in Fig. 2, where the temperature rise in the combustion zone of a well-stirred reactor is plotted over the preheat temperatures.

Principle of a Flameless Oxidation Burner

As mentioned before, a furnace is only able to run flameless oxidation at temperatures above 800 °C. To heat up the combustion chamber, a starting burner is needed. Fig. 3 shows the principle of a flameless oxidation burner, which can be operated in a stable flame mode as well as in a flameless oxidation mode. The burner used for this investigation is a REKUMAT-Burner of WS-Wärmeprozesstechnik with a built-in heat exchanger for air preheating.

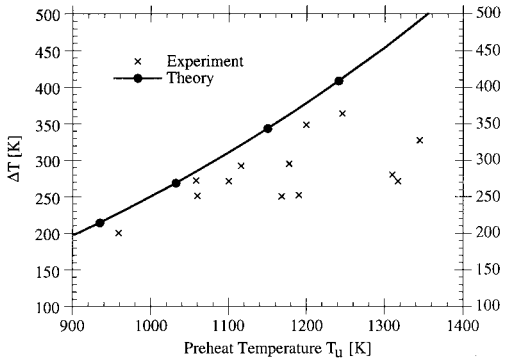

FIG. 2. Temperature rise ΔT in the reaction zone shown as function of preheat temperature T_u for a well-stirred reactor with monotonous transition between the burnt and unburnt state compared with measurements from flameless oxidation.

During the process of heating up the furnace, fuel (1) is led into a combustion volume within the burner (2) and mixed with air (3). The mixture is electronically ignited, and six burner-stabilized flames are formed to heat up the furnace. Fig. 4 shows the temperature and NO_x emissions during the start-up. The exhaust gases stream, due to the furnace geometry, in a reverse flow and are guided outward of the furnace along (5) the heat-exchanging fins of the burner. The exhaust gases heat up the air and accelerate its flow velocity. Once the chamber has reached a temperature above 800 °C, safe operation for flameless oxidation mode is possible, and a control valve (8) switches the fuel flow to the center nozzle (9). The stable flames extinguish, and the air with its high momentum is diluted with the recirculating flue gases. A mixture between exhaust gases, air, and fuel is formed and heated up continuously by the hot gases. A reaction takes place further downstream in the furnace. Suddenly, the NO_x emissions decrease significantly, as can be seen in Fig. 4. Fig. 5 shows a comparison along the centerline of temperature between the flame-stabilized and flameless oxidation modes at a constant chamber temperature of 1275 K. The chamber temperature was measured at the bottom of the combustion chamber close to the wall to ensure safe operating conditions. Whereas the temperature for the burner-stabilized mode is very high at the burner ($x/L = 0.$) and decreases with distance from the burner, the temperature of the flameless oxidation mode is low at the burner and increases continuously to temperatures of about 1200 K.

Experimental Apparatus and Applied Techniques

The experimental apparatus consisted mainly of a tunable excimer laser (Lambda Physik EMG 150

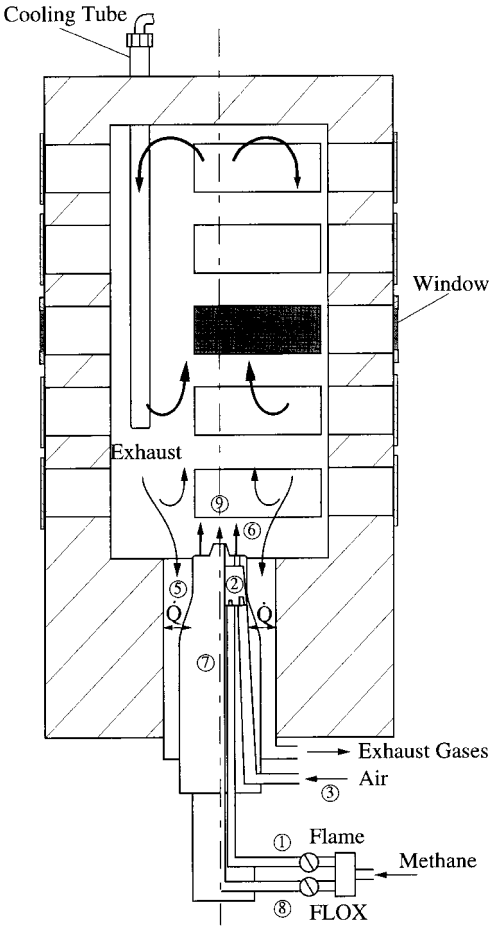

FIG. 3. Principle of a burner and combustion chamber used for flameless oxidation.

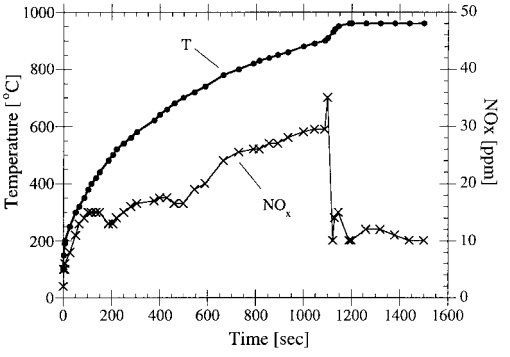

FIG. 4. Starting behavior of a flameless oxidation burner. At $T = 800$°C, the burner switches from stable flame mode to flameless oxidation mode; as a result, NO_x emissions decrease significantly.

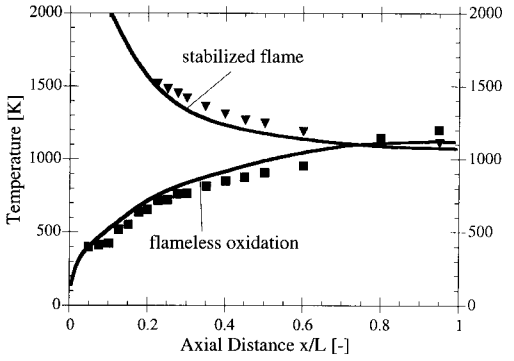

FIG. 5. Comparison of temperature along the centerline of the combustion chamber between flame-stabilized and flameless oxidation mode at a constant chamber temperature of 1275 K. Temperatures were obtained experimentally from thermocouple measurements and numerically [1].

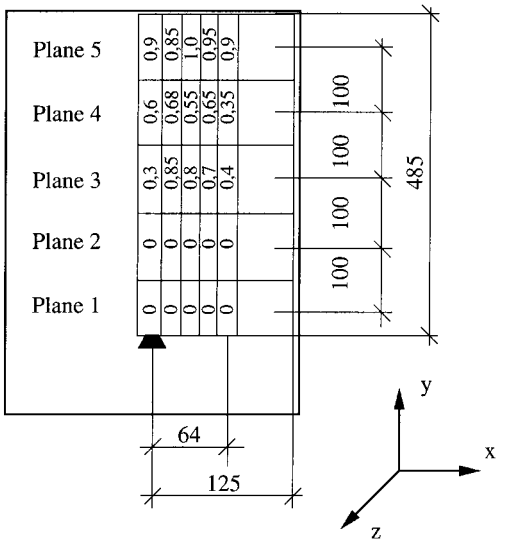

FIG. 6. Located areas of combustion (1 = always OH signal; 0 = no OH signal). Reaction starts from level 3, where local temperatures in the unburnt gases are above 950 K.

TMSC), two intensified water-cooled ICCD camera systems, and an optically accessible combustion chamber for flameless oxidation, which is described in Ref. [5]. For the comparison of flameless oxidation to premixed combustion, the flameless oxidation chamber was replaced by a Bunsen burner for turbulent flames, as reported in detail in Ref. [6]. Symmetry was assumed so that the area of interest could be reduced to one-fourth of the chamber. The chamber was divided into five vertical planes. Only in the investigated planes fused-silica windows were introduced. The other windows were sealed to minimize heat loss. The process heat was exchanged with an air-cooled rod. Rayleigh scattering and OH fluorescence images were collected perpendicular to the incident laser sheet that was focused with a single cylindric lens ($f = 300$ mm). A MgF_2 plate was used to turn the polarization to maximize the Rayleigh signal. The signals were separated with a long pass mirror so that the inelastic scattered Rayleigh signals could be collected with an interference filter (bandwidth, 8 nm) by one ICCD camera. The second ICCD camera was used for OH imaging. A Schott UG11 glass filter was chosen to discriminate between the OH signal around 298 nm and other wavelength signals. For time controlling of the experiment, a pulse delay generator was used.

Laser-Induced Predissociative Fluorescence of the OH Radical

The UV laser beam was tuned to 248.457 nm. At this wavelength, the OH radical is excited over the $P_2(8)$ transition in the $[A^2\Sigma^+ \leftarrow X^2\Pi(3,0)]$-band system. It provides strong fluorescence of the OH radical due to the high spectral energy, although predissociation ($P \approx 10^{10}$ s^{-1}) occurs faster than quenching ($Q \approx 6 \times 10^8$ s^{-1}) and much faster than fluorescence ($A \approx 10^6$ s^{-1}) [7]. The collected intensity of OH I_F can be denoted as

$$I_F = c_{opt} \frac{A}{P} I_L[N_{OH}] f_B(T) \qquad (3)$$

This means that quenching can be neglected and the emitted laser-induced predissociative fluorescence intensity I_F is proportional to the number density of OH $[N_{OH}]$ in the excited volume and the laser intensity I_L. $f_B(T)$ is the Boltzmann distribution and c_{opt} an optical constant representing the collection and quantum efficiency of the optical system.

Rayleigh Thermometry

The gas temperature within the chamber was calculated from the measured Rayleigh images. The Rayleigh intensity I_{Ray} is inversely proportional to the fourth power of the wavelength λ ($I_{Ray} \sim 1/\lambda^4$) and depends on laser energy I_L, an optical constant, collection angle, number density, and a Rayleigh cross section σ [8]. The Rayleigh cross section is assumed to be constant over the reaction zone because high dilution of the unburnt mixture with exhaust gases changes the cross section no more than 2% between the unburnt and burnt gases. The Rayleigh intensity is calculated from the measured signal I_m by

$$I_m = I_{Ray} + I_{Background}(T_{chamber}) \qquad (4)$$

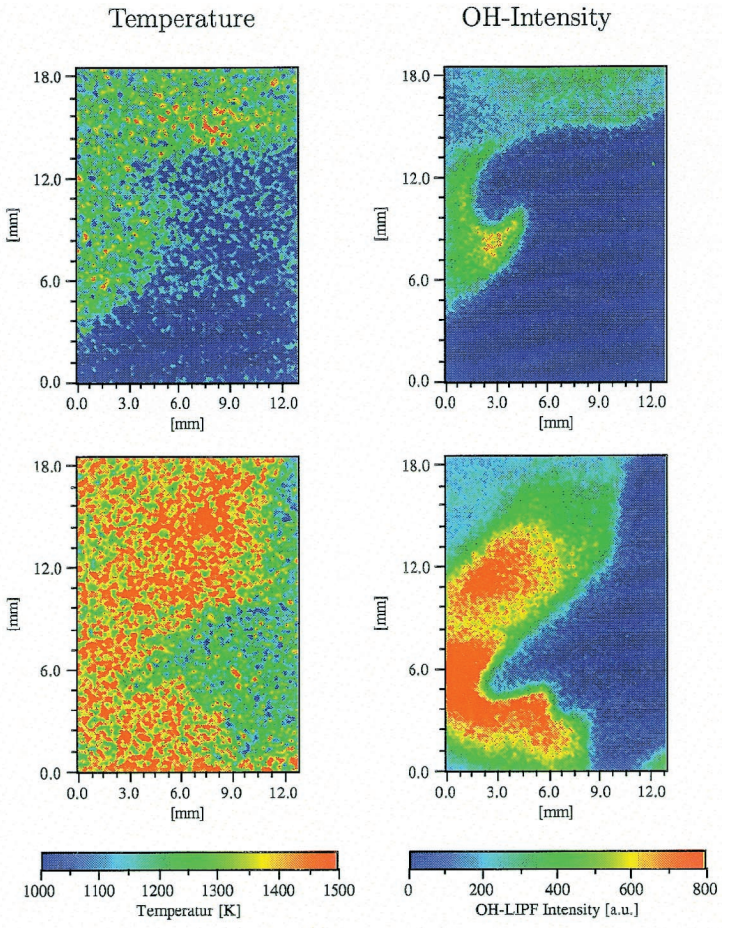

FIG. 7. Selected simultaneously taken temperature and OH-LIPF images of flameless oxidation (all images from fourth plane, center position).

The background intensity $I_{\text{Background}}$ was measured and decreases significantly with increasing chamber temperature, because the reflectivity of the insulating material in the chamber changes with temperature. To eliminate optical constants, the temperature T_{Ray} is calculated with a reference image at a known temperature T_{ref}:

$$T_{\text{Ray}} = \frac{I_{\text{Ray}_{\text{ref}}}}{I_{\text{Ray}}} \frac{\sigma_i}{\sigma_{\text{ref}}} \frac{I_{\text{L}}}{I_{\text{L}_{\text{ref}}}} T_{\text{ref}} \qquad (5)$$

Data Reduction

The Rayleigh and OH images were matched and checked for distortion by imaging a fine grid wire (0.16-mm wire thickness and 0.5-mm spacing). For OH-LIPF signals, no quantitative correction was made to remove the fluorescence signals from the lower vibrational states ($v' = 0, 1, 2$). It is the qualitative behavior of OH radicals that will be discussed later. Image smoothing based on convolution theory has been applied twice to each instantaneous image to reduce the noise in each image. The smoothing size is chosen to be less than the smallest physical length scale (laminar flame thickness ~0.15 mm). Errors in the temperature measurements were analyzed to be no more than 11%.

Operating Conditions

The combustion chamber was operated with a power of approximately 10 KW using methane and air in a stoichiometric mixture. The chamber temperature was held constant at 900 °C during operation in the flameless oxidation mode, whereas the air was preheated up to 500 °C. Typical NO_x emissions were below 10 ppm (see Fig. 4). Mean exit velocities were 67 m/s for air and 20 m/s for methane.

Results and Discussion

Visualization of Combustion

For the visualization of the combusting areas within the chamber, at each position of the chamber,

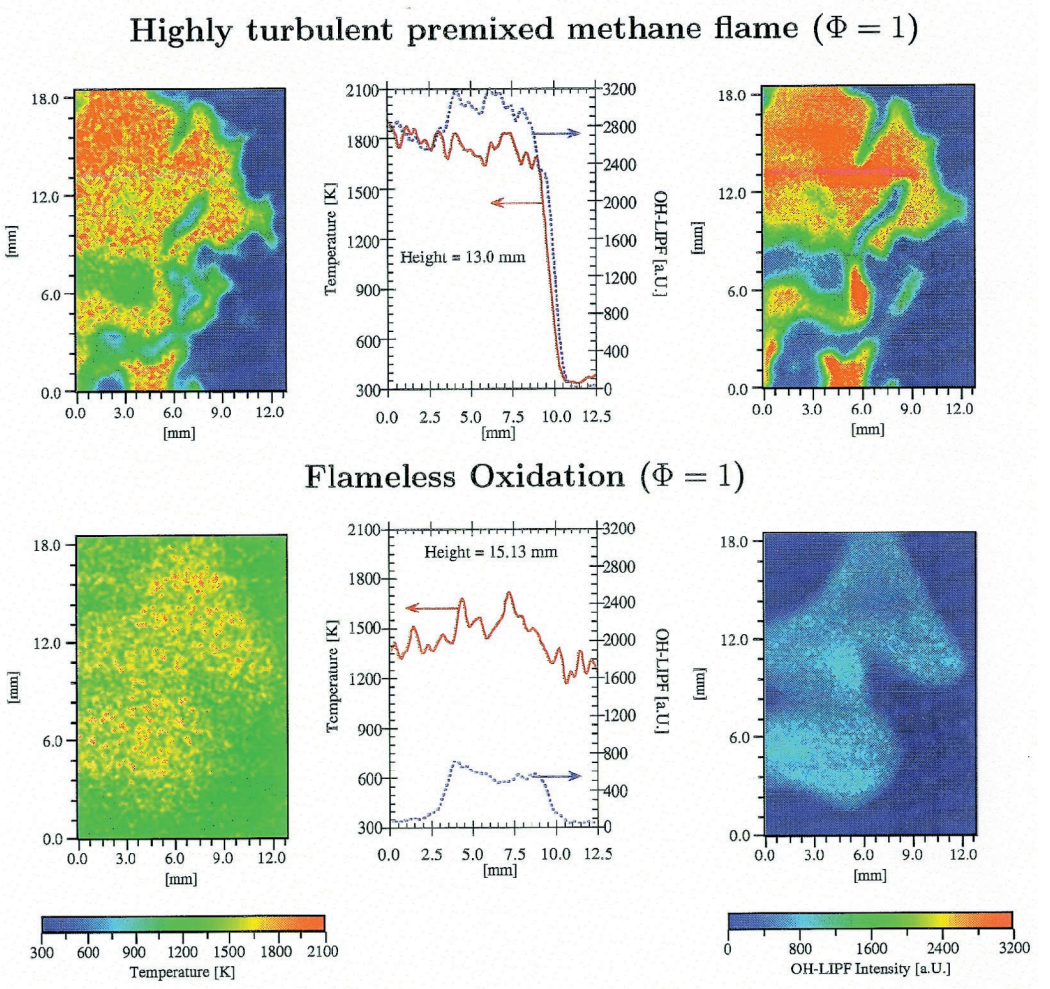

FIG. 8. Comparison of simultaneously taken temperature and OH-LIPF images between premixed flames under highly turbulent condition and flameless oxidation.

30 OH-LIPF images were taken. A reaction probability was calculated from these images by dividing the number of images with OH detection by the total number. The result is depicted in Fig. 6. Combustion could be observed only in the upper three planes. Along the centerline, less reaction was detected than in the middle of the investigated positions. In the fourth plane, less reaction could be detected than in the third and the fifth planes. This is probably due to the low statistical accuracy of 30 images per position. In the first two imaging planes above the burner, no OH-LIPF signal could be detected. In these first two planes, the measured Rayleigh images showed that mixing between fuel, air, and exhaust gases was still going on and that the temperature was not high enough for combustion to take place. This agrees well with thermocouple temperature measurements along the centerline shown in Fig. 5, which are compared with numerical calculations [1]. At a distance of $x/L = 0.3$ (L is length of combustion chamber), temperatures are high enough to ignite the diluted premixture. Reaction was detected from OH-LIPF at temperatures above 950 K in the unburnt gases. Fig. 7 shows as an example two simultaneously taken image pairs of OH-LIPF and temperature from the fourth plane at the central position. Combustion occurs in disconnected reaction zones in which the temperature and OH-signal intensities differed substantially. This is due to varying amounts of recirculated flue gases. Fig. 2 shows the measured temperature rise in the reaction zone as a function of preheat temperature. Maximum temperatures, averaged over 10 × 10 pixel,

were measured up to 1650 K, whereas the temperature rise in the reaction zone with respect to the preheated unburnt mixture differed between 200 and 400 K. All temperature rises in Fig. 2 are below the solid line for monotonous transition between the burnt and unburnt state. The scattering of the experimental results are due to the varying amounts of flue gases in the unburnt mixture. It can be concluded that flameless oxidation takes place in the region of a well-stirred reactor where no ignition and quenching events occur, which is why no combustion noise occurs.

Comparison to Turbulent Premixed Combustion

For the analysis of the structure of flameless oxidation, a comparison to premixed combustion is chosen. Measurements were done in a wrinkled, low-turbulent and in a high-turbulent premixed methane Bunsen flame, which is compared with measurements in the flameless oxidation chamber (detailed information about the Bunsen flame is in Ref. [6]). Fig. 8 shows simultaneous measurements of OH-LIPF and temperatures. On the left-hand side, the temperature is located, and on the right-hand side, the OH-LIPF images are located. In between the OH and temperature images, representative horizontal sections of the reaction zones at the indicated height are shown. All images were taken under exactly the same optical conditions. In a wrinkled premixed flame (not shown in Fig. 8), a sharp rise of temperature and OH in the reaction zone could be observed, which is typical for the flamelet structure [4]. The maximum of OH occurs in the vicinity of the thin reaction zone. In the oxidation zone downstream, the OH signal decreases continuously. The highly turbulent premixed flame (upper images in Fig. 8) shows a very sharp temperature rise of about 1500 K within the reaction zone, similar to that in a wrinkled flame. However, the OH distribution becomes more uniform in the burnt side, because turbulence is affecting the oxidation zone. In the case of flameless oxidation, there is only a small temperature rise, temperatures stay below 1650 K, and the OH intensity is significantly lower. The OH intensity shows a homogeneous distribution on the burnt side similar to the structure of highly turbulent premixed flames, although less wrinkling of the reaction zone indicates a less turbulent state. The dilution with exhaust gases increases the chemical timescales compared with the turbulent timescales. A further detailed investigation of the turbulent parameters will be needed for a complete analysis and classification of flameless oxidation.

REFERENCES

1. Wünning, J. A. and Wünning, J. G., *Prog. Energy Combust. Sci.* 23(12):81–94 (1997).
2. Flamme M., *Gaswärme International* 41(10):438–444 (1992).
3. Wünning, J., *Chem.-Ing.-Tech.* 63(12):S1243–S1245 (1991).
4. Peters, N., *Fifteen Lectures on Laminar and Turbulent Combustion,* Ercoftac Summer School, RWTH Aachen, September 14–25, 1992.
5. Plessing, T., Wünning J. G., and Peters, N., 18. *Deutsch-Niederländischer Flammentag,* VDI-Berichte 1313, 1997, pp. 537–542.
6. Chen, Y. C., Peters, N., Schneemann, A., Wruck, N., Renz, U., and Mansour, M. S., *Combust. Flame* 107:223–244 (1996).
7. Rothe, E. W. and Andresen, P., *Appl. Optics* 36(18):3971–4033 (1997).
8. Eckbreth, A. C., *Laser Diagnostics for Combustion Temperature and Species,* Abacus Press, Cambridge, 1988.

COMMENTS

Gus Nathan, University of Adelaide, Australia. Have you compared the heat-transfer characteristics of FLOX with a conventional burner?

Author's Reply. The occurrence of luminosity in non-sooting flames depends on the electronic excitation of radicals such as CH and C_2, which depends strongly on temperature. The wavelength of the luminosity in the visible range occurs around 400 nm and gives the flame a bluish color. It has no impact on the heat transfer, mostly governed by thermal radiative transfer. In flameless oxidation (FLOX), the temperature distribution is more uniform in the furnace, which enhances the heat transfer. However, absolute temperatures are lower in the flame region, resulting in less thermal radiation. Overall, no significant difference in heat-transfer characteristics can be observed.

•

Antonio Cavaliere, University of Naples, Italy. Did you measure any other spectral characteristics from spontaneous or laser-excited emissions, which show the presence of species different from OH? Such observations would be relevant in understanding this "new" oxidation phenomena.

Author's Reply. We tried to image reaction zones with LIF measurements of C_2H_Y molecules and did not find any signal in the reactive areas even at fuel-rich conditions. This indicates that at flameless oxidation, the combustion of CH_4 does not involve C_2 chemistry.

•

A. K. Gupta, University of Maryland, USA. Fuel property has a strong effect on the structure and emission spectra of highly preheated air flames. Changing the fuel from methane to propane changes the emission spectra of flames and transforms the colorless flame to a flame with color [1].

REFERENCE

1. Bolz, S and Gupta, A. K., International Joint Power Generation Conference, Baltimore, MD, August 1998.